(LNS Experiment : #2467)

Study of Giant Resonances in the ^{24}Mg (e, e′α) Reaction

K. Takahashi[1*], K. Abe[1], R. Hashimoto[2], Y. Hayashi[2], K. Hirose[1], T. Ishikawa[2], H. Kanda[1], K. Maeda[1], H. Miyase[1], I. Nishikawa[2], Y. Sato[2], T. Tamae[2], H. Tsubota[1], M. Utoyama[1], M. Wakamatsu[1], M. Watabe[2], Y. Yamaguchi[1]

[1]*Physics Department, Graduate School of Science, Tohoku University, Aramaki, Aoba-ku, Sendai 980-0845*
[2]*Laboratory of Nuclear Science, Tohoku University, Mikamine, Taihaku-ku, Sendai 982-0826*

§1. Introduction

The giant resonances in light nuclei have been investigated by the (e, e′α) reaction in several nuclei. In ^{12}C and ^{40}Ca, where the (e, e′α) reaction through the $E1$ transition is considered to be forbidden by the isospin selection rule because these are $Z = N$ nuclei. The reported $E1$ strength was very small or neglected and the $E2$ or $E0$ strength was dominant [1,2]. Concerning the $E0$ excitation, there are intensive studies by alpha scattering with the intention to find the isoscalar giant monopole resonance (ISGMR) [3-8]. The ISGMR is interesting with regard to the compressibility of nuclear matter. Considering that the (e, e′α) reaction occurs only through isoscalar resonances, the (e, e′α) reaction can be an alternative tool for searching the ISGMR. However, only a fraction of the ISGMR strength is related to α emission channels, although one can reconstruct the strength by using the statistical model for example [2].

This work reports an investigation of the excitation and decay of the giant resonances in ^{24}Mg (e, e′α) reaction.

§2. Experiment

The experiment was performed at Laboratory of Nuclear Science (LNS) in Tohoku University at an incident energy of E_0 =199.31MeV and a scattering angle of $\theta_e = 30^\circ$, corresponding to a momentum transfer of $q = 0.51$ fm^{-1}, using a continuous electron beam from the Stretcher-Booster Ring. A typical electron current during the experiment was from 0.5 to 1 μA.

A ^{24}Mg foil of 2mg/cm^2 and 99.99% enriched was used as a target. The thickness was fixed so that the energy loss of emitted α particles in the target is not too large. The scattered electrons were detected by is a double-focusing magnetic spectrometer with a solid angle of 6 msr. A vertical drift chamber (VDC) was used for detecting the electrons on the focal plane of the spectrometer. Three layers of plastic scintillator were set behind the VDC for trigger of data acquisition. With 5 % of acceptance of the spectrometer, the range of the excitation energy was 15-25 MeV. In this energy range, proton, deuteron, triton, and α particles can contribute to the charged particle decay. The range was chosen

*Present address: ART KAGAKU Co.,Ltd, Muramatsu, Tokai-mura, Naka-bun, Ibaraki 319-1112

because the α decay strength of ^{24}Mg (e, e′α) reaction was very small around 20 MeV or higher according to previous experiments.

Emitted charged particles were detected in coincidence with scattered electrons by using 12 SSD telescopes which consists of two layers of SSD. The first SSD was 50 μm thick and the second was 1 mm thick. These telescopes were placed in a plane rotated about q axis by ϕ =90°. With the out-of-plane detection, the telescopes were able to be arranged without disturbing the electron beam and scattered electrons. Furthermore, an analysis is easier because the longtudinal-transverse interference term vanishes.

§3. Experimental Results and Analysis

Figure 1 shows an example of the missing energy spectrum. According to the Bethe-Bloch formula, the energy loss of α particles in the target is not negligible. So it was taken into account assuming that the emitted particles pass a half of the target thickness.

The separation of α_0 and α_1 events were done by fitting two components of α_0 and α_1 generated by calculation to the experimental spectrum as shown in Fig. 2, because the energy resolution was not enough to separate the peaks clearly. A function used for the fitting is

$$g(E_{\mathrm{miss}}) = a_0 f_{\alpha 0}(E_{\mathrm{miss}} - b, \sigma) + a_1 f_{\alpha 1}(E_{\mathrm{miss}} - b, \sigma) + c, \quad (1)$$

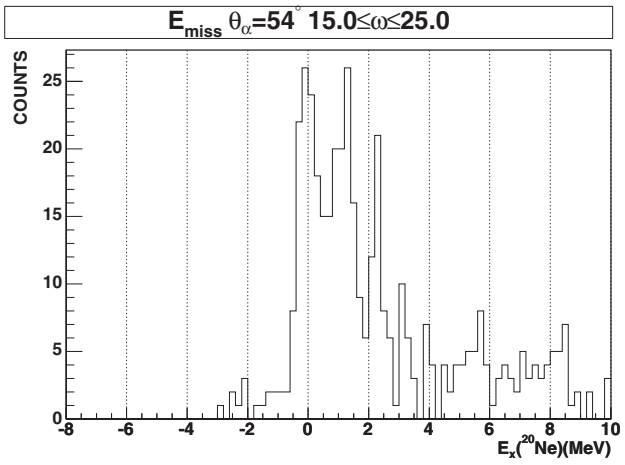

Fig. 1. Missing energy spectrum for excitation energys from 15 to 25 MeV. The excitation energy of the first excited state is 1.14 MeV. It was corrected for the energy loss in the target using the Bethe-Bloch formula by assuming that particle emissions started at the center of the target.

where $f_{\alpha 0}$ and $f_{\alpha 1}$ are functions for the contributions of α_0 and α_1, individually, generated by calculation; E_{miss} is the missing energy, σ is the energy resolution of each of SSD telescopes, and a_0, a_1, b, c are free parameters. Considering low quality of statistics of our data, the most likelihood method was used for fitting by utiliyzing MINUIT for maximization of the likelihood [9].

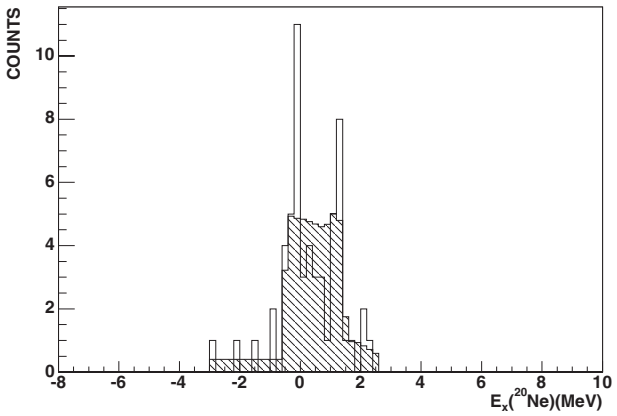

Fig.2. Fitting of the missing energy spectrum with the spectrum generated by the calculation. Hatched histogram is the sum of the calculations fitted with α_0, α_1 and the background. The calculation takes into account the initial energy of α, the energy loss while passing through the target, and the resolution of detectors.

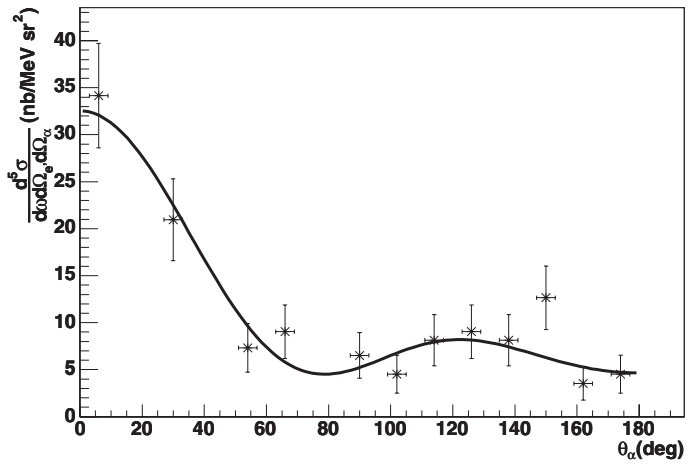

Fig.3. Angular distribution of α_0 for excitation energies of 15-16.4 MeV. The solid line shows a result of fitting by Eq.(2).

Figure 3 shows the angular distribution of the (e, e′α_0) reaction extracted by the method described above. The curve in the figure shows the angular correlation function which we discuss later.

§4. Discussion

In case of spin and parity of $J^\pi = 0^+$ for all of the target, residual nucleus, and emitted particle, the

(e, e′α) differential cross section with multipolarities up to 3 can be simplified as following [10]:

$$\frac{d^5\sigma}{d\omega d\Omega_{e'} d\Omega_{\alpha_0}} = \sigma_{\mathrm{Mott}} \left| \sum_{L=0}^{3} \sqrt{(2L+1)\,A_0(L)}\, F_{CL}\, e^{i\delta L} P_L(\cos\theta_{\alpha_0}) \right|^2, \tag{2}$$

where σ_{Mott} is the Mott cross section, F_{CL} is the longitudinal electric form factor, $A_0(L)$ is the decay coefficient, δ_L is the phase of the product of F_{CL} and $A_0(L)$. Taking $\sqrt{(2L+1)\,A_0(L)}\,F_{CL}$ and δ_L as free parameters, fitting by χ^2 minimization was performed. In the ^{24}Mg (e, e′ α_0) reaction, the angular momentum of the excited state J is defined unambiguously as equal to L because spins of the ground state of the residual nucleus and the emitted particle are zero. Concerning the upper limit of multipolarity in Eq.(2), $L \leq 2$ or $L \leq 3$ is adequate. In the ^{26}Mg (e, e′ α) experiment [10], its momentum trasfers are 0.35 and 0.54 fm^{-1}, that are very close to ours. The $E3$ component was not included in the multipole decomposition because it was supposed to be negligible by the DWBA calculation. It was not included also in ^{40}Ca (e, e′ α) experiment [2]. In those results, there is a discrepancy between the experimental angular distribution and the fitted curve at 0°. On the other hand, the result of the ^{12}C (e, e′ α) experiment [1] at in $q = 0.24$-0.61 fm^{-1} shows a relatively better fitting result at 0° by including the $E3$. Furthermore, 39% of the $E3$ EWSR (energy weighted sum rule) has been found in ^{24}Mg (e, e′) reaction. Considering these facts, we included the $C3$ component by defining $L \leq 3$ in Eq.(2). The solid line in Fig. 3 is the result of fitting by χ^2 minimization.

Using the parameters obtained by the fitting, the cross section for each multipolarity is given by

$$\frac{d^5\sigma_L}{d\omega d\Omega_{e'}} = \sigma_{\mathrm{Mott}}(2L+1)\,A_0(L)\,|F_{CL}|^2 \int \left[P_L(\cos\theta_{\alpha_0})\right]^2 \mathrm{d}\Omega_{\alpha_0}. \tag{3}$$

Using the values obtained from the fitting, we deduced the strength function $B_{CL}(q)$ which can be represented for spin 0 nuclei by the first Born approximation as follows [11],

$$B_{CL}(q) = \frac{d\sigma_{CL}}{d\Omega_{e'}} \left\{ 4\pi\sigma^1_{\mathrm{Mott}} \left(\frac{\Delta^2}{q^2}\right)^2 f_{\mathrm{rec}}\, q^{2L} [(2L+1)!!\,]^{-2} \right\}^{-1} \tag{4}$$

for $L \geq 1$, and

$$B_{C0}(q) = \frac{d\sigma_{C0}}{d\Omega_{e'}} \left\{ 4\pi\sigma^1_{\mathrm{Mott}} \left(\frac{\Delta^2}{q^2}\right)^2 f_{\mathrm{rec}}\, q^4 [15]^{-2} \right\}^{-1} \tag{5}$$

for $L = 0$, where σ^1_{Mott} is the Mott cross section for $Z = 1$, $\Delta^2 = q^2 - \omega^2$, and f_{rec} is described by

$$f_{\mathrm{rec}} \sim \left[1 + \frac{2k_1}{M} \sin^2\frac{\theta}{2}\right]^{-1}. \tag{6}$$

Furthermore, $B_{CL}(q)$ can be expanded as following,

$$\left(\frac{B_{CL}(q)}{B_{CL}(q=0)}\right)^{\frac{1}{2}} = 1 - \frac{q^2 < r^2_{CL} >_{\mathrm{tr}}}{2(2L+3)} + \frac{q^4 < r^4_{CL} >_{\mathrm{tr}}}{8(2L+3)(2L+5)} - \cdots\cdots, \tag{7}$$

$$< r^{l}_{CL} >_{\rm tr} = \frac{\int r^{L+l+2}\,\rho_L(r)dr}{\int r^{L+2}\,\rho_L(r)dr}\ , \tag{8}$$

for $L \geq 1$, and

$$\left(\frac{B_{C0}(q)}{B_{C0}(q=0)}\right)^{\frac{1}{2}} = 1 - \frac{q^2 < r^2_{C0} >_{\rm tr}}{20} + \frac{q^4 < r^4_{C0} >_{\rm tr}}{840} - \cdots\cdots, \tag{9}$$

$$< r^{l}_{C0} >_{\rm tr} = \frac{\int r^{l+4}\,\rho_0(r)dr}{\int r^{4}\,\rho_0(r)dr} \tag{10}$$

for $L = 0$. $\rho_L(r)$ is the transition charge distribution which is described by Tassie model [12],

$$\rho_L(r) \propto r^{L-1}\frac{d\rho_{\rm g.s.}(r)}{dr} \tag{11}$$

for $L \geq 1$, and

$$\rho_0(r) \propto 3\,\rho_{\rm g.s.}(r) + r\,\frac{d\,\rho_{\rm g.s.}(r)}{dr} \tag{12}$$

for $L = 0$, where $\rho_{\rm g.s.}(r)$ is the charge distribution for the ground state described by the three parameter Fermi model,

$$\rho_{\rm g.s.}(r) = \left(1 + \frac{\omega r^2}{t^2}\right)\left(1 + \exp\left(\frac{r-c}{t}\right)\right)^{-1}. \tag{13}$$

In Eq.(13), we used parameters

$$(\omega, c, t) = (-0.249,\ 3.192,\ 0.604) \tag{14}$$

according to Ref. [12].

$B_{CL}(q=0)$ for individual multipolarities was obtained by calculating the right-hand side of Eqs. (7) and (9) for $q = 0.51$ fm^{-1}, and applying $B_{CL}(q)$ given by Eqs. (4) and (5). Eventually, the strength at the photon point, $B_{CL}(q=\omega)$ was obtained by substituting the $B_{CL}(q=0)$ to Eq. (7) or (9).

Using the $B_{CL}(q=\omega)$ obtained above, the fraction of the energy weighted sum rule (EWSR) is given by

$$R = \frac{B_{CL}(\omega)\,\omega}{EWSR(EL,\,\Delta T)} \times 100, \tag{15}$$

where values of the EWSR are given as follows [13],

$$S(E0) = \frac{(2\hbar)^2}{m_p}\ \frac{Z^2}{A} < r^2 >\ ,$$

$$S(E1, \Delta T{=}1) = \frac{9\hbar^2}{8\pi m_p} \frac{NZ}{A},$$

$$S(EL, L > 1) = \frac{L(2L{+}1)^2\hbar^2}{8\pi m_p} \frac{Z^2}{A} < r^{2L-2} >, \quad (16)$$

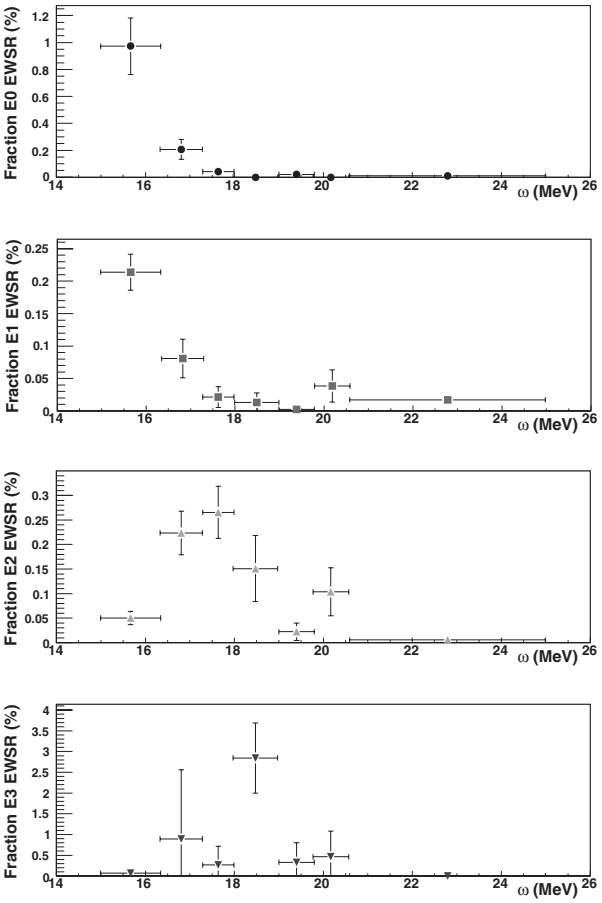

Fig.4. Fraction of the energy weighted sum rule for individual multipolarities.

Figure 4 displays the fraction of the EWSR obtained by Eq. (15), and the result is summarized in Table 1 with results of other experiments. Most of the strength was detected between 15 and 20 MeV. It must be affected by competition between various decay channels. Actually the $E0$ strength with 1.2% of the $E0$ EWSR was detected, while α scattering [6] found 72% with the centroid energy of 21 MeV. The $E1$ strength with 0.4% of the $E1$ EWSR was found, which is comparative with the (α, γ_0) reaction, and very small comparing with the (γ, p_0) reaction. This is the effect of the suppression by the isospin selection rule. The $E2$ strength with 0.8% of the $E2$ EWSR was found. Its distribution is similar to (α, γ) [14] reaction although the amount is different.

In the analysis of electron scattering [15], the separation of $E0$ and $E2$ was not possible by principle.

Table 1. Summary of strength obtained by this work and other experiments on ^{24}Mg.

$L \geq$	experiment	ω (MeV)	R (% EWSR)
0	^{24}Mg(e, e'α_0)	15.0-25.0	1.2 ± 0.2
0	^{24}Mg(α, α)[6]	0-41	72 ± 10
0	^{26}Mg(e, e'α_0)[10]	14.0-26.0	0.2
1	^{24}Mg(e, e'α_0)	15-25	0.4 ± 0.1
1	^{24}Mg(e, e')[15]	9.0-34.0	84.9
1	^{24}Mg(e, α_0)[16]	13.5-22.5	0.43
1	^{24}Mg(γ, p_0)[17]	15.1-23.0	3.3
1	^{24}Mg(γ, n)[18]	16.5-28.0	14.0
1	^{20}Ne(α, γ_0)[14]	14.6-20.6	0.33
1	^{24}Mg(α, α)[6]	0-41	81^{+26}_{-14}
1	^{26}Mg(e, e'α_0)[10]	14.0-26.0	0.45
2	^{24}Mg(e, e'α_0)	15-25	0.8 ± 0.1
2	^{24}Mg(e, e')[15]	0.0-34.0	117
2	^{24}Mg(e, α_0)	13.5-22.5	6.0 ± 0.5
2	^{20}Ne(α, γ_0)[14]	12.0-22.5	11.8 ± 1.0
2	^{24}Mg(α, α)[6]	0-41	72 ± 10
2	^{26}Mg(e, e'α_0)[10]	14.0-26.0	1.4
3	^{24}Mg(e, e'α_0)	15-25	4.8±2.1
3	^{24}Mg(e, e')[15]	0.0-34.0	115
3	^{24}Mg(α, α)[6]	0-41	31^{+9}_{-6}

Figure 5 shows comparison between the $C2(C0)$ differential form factor from (e, e′) inelastic scattering and our results of $C0$ and $C2$ differential cross sections. Comparison is limited to the excitation energies below 20 MeV because the cross sections in our data are small above it. There is a peak around 15 MeV in the (e, e′) reaction. The $C0/C2$ ratio is estimated from the present experiment as $C0/C2=5$ for the corresponding energy bin (15 ～ 16.4 MeV). For a peak between 16 and 18 MeV observed in the (e, e′) reaction the present result represents that $C2$ is dominant. The $C0/C2$ ratio is obtained as $C0/C2 = 0.9$ between 16.4 ～ 17.3 MeV, and $C0/C2 = 0.15$ between 17.3 and 18.0 MeV from our data.

Concerning the $C3$, the strength was 4.8% of the $E3$ EWSR. The validity of including $E3$ can be provided from the q dependence of the form factor investigated in the inelastic scattering experiment. In the inelastic scattering experiment, a significant amount of $E3$ strength was detected at $q = 0.73$ fm^{-1}. According to the q dependence, the $C3$ strength at $q = 0.51$ fm^{-1} (our experiment) is smaller than $C3$ at $q = 0.73$ fm^{-1} by a factor of 4. This difference is not too large to expect the presence of that at $q = 0.51$ fm^{-1}. Furthermore, we compared the ratio $C3/C2$ of the inelastic scattering data and of our work. The strength was reconstructed by the method of statistical model when calculating the ratio for our work. Then we obtained $C3/C2=0.35$ for the inelastic scattering data and 0.48 for our work in the range of

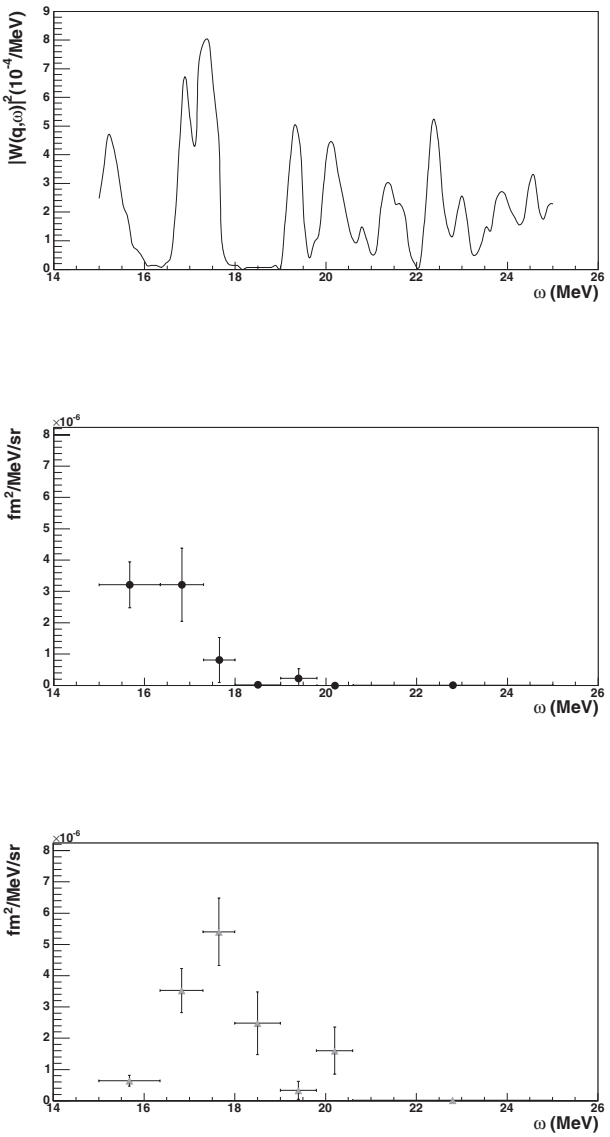

Fig.5. The Differential form factor of $C2(C0)$ at $q=0.73$ fm^{-1} from (e, e') experiment [15](top), differential cross section of $C0$ (middle), and $C2$ (bottom) of our expemriment.

15-19.8 MeV.

In the same manner, we compared the $C1/C2$ ratio in order to examine how much the C1 suppression can be seen. It was 1.79 for the inelastic scattering data and 0.79 for our work, that means the isospin mixing occured with the rate of 44%. That is 24% in the (e, α) [10] and (α, γ) [14] experiments.

§5. Conclusion

The ^{24}Mg(e, e'α) experiments was performed at $q=0.51$fm^{-1} and in the range of excitation energy of 15-25 MeV.

From analysis of the angular distribution for α_0 channel, the $C0$, $C1$, $C2$ and $C3$ form factors were

decomposed to obtain the strength distribution for each multipolarity. The $C0$ and $C2$ components, which was not able to be decomposed by (e, e′) data, were separated and the result indicated that the $C0$ excitation is dominant around 15-16 MeV and the $C2$ ($C0$) peak at 17 MeV found in the (e, e′) experiment is identified to be $C2$ from our result. From the comparison of the $C1/C2$ ratio for the data with (e, e′) result, it was found that the isospin mixing occurs with the rate of 41% in the $E1$ excitation. In our multipole decomposition, the $C3$ component was included that was sometime igonored or neglective in previous studies. Comparing the $C3/C2$ ratio with the (e, e′) result, the $C3$ strength which we obtained is thought to be reasonable. The $C1$ suppression by the isospin selection rule probably makes the $C3$ easier to be identified. Although it was clear that only a fraction of strength can be seen in the (e, e′α) reaction, the coincidence experiment can decompose the $C0$ and $C2$ components. Better statistics is required to discuss more precisely.

References

[1] D.J. DeAngelis, J.R. Calarco, J.E. Wise, H.J. Emrich, R. Neuhausen, and H. Weyand: Phys. Rev. C**52** (1995) 61.

[2] M. Kohl, P. von Neumann-Cosel, A. Richter, G. Schrieder, and S. Strauch: Phys. Rev. C**57** (1998) 3167.

[3] D.H. Youngblood, C.M. Rozsa, J.M. Moss, D.R. Brown, and J.D. Bronson: Phys. Rev. Lett. **39** (1977) 1188.

[4] Y.W. Lui, J.D. Bronson, D.H. Youngblood, Y. Toba, and U.Garg: Phys. Rev. C**31** (1985) 1643.

[5] S. Shlomo and D.H. Youngblood: Phys. Rev. C**47** (1993) 529.

[6] D.H. Youngblood, Y.-W. Lui, and L. Clark: Phys. Rev. C**60** (1999) 014304.

[7] D.H. Youngblood, H.L. Clark, and Y.-W. Lui: Phys. Rev. C**65** (2002) 034302.

[8] B. John, Y. Tokimoto, Y.-W. Lui, H.L. Clark, X. Chen, and D.H. Youngblood: Phys. Rev. C**68** (2003) 014305.

[9] F. James: CERN Program Library Long Writeup D506.

[10] L.A.A. Terremoto, V.P. Likhachev, M.N. Martins, H.J. Emrich, G. Fricke, Th. Kröhl, and K.W. Neff : Phys. Rev. C**56** (1997) 2597.

[11] T. deForest Jr. and J.D. Walecka: Adv. Phys. **15** (1966) 1.

[12] L.J. Tassie: Austr. J. Phys. **9** (1956) 407.

[13] R. Pitthan, F.R. Buskirk, W.A. Houk, and R.W. Moore: Phys. Rev. C**21** (1980) 28.

[14] E. Kuhlmann, E. Ventura, J.R. Calarco, D.G. Mavis, and S.S. Hanna: Phys. Rev. C**11** (1975) 1525.

[15] K. Itoh, S. Osawa, Y. Torizuka, T. Saito, and T. Terasawa: Phys. Rev. C**23** (1981) 945.

[16] M. Hirooka, T. Tanaka, T. Hino, A. Tanaka, T. Tamae, M. Sugawara, and M. Miyase: Nucl. Phys. **A431** (1984) 269.

[17] R.C. Bearse, L. Meyer-Sch\ützmeister, and R.E. Segel: Nucl. Phys. **A116**, (1968) 682.

[18] S.C. Fultz, R.A. Alvarez, B.L. Berman, M.A. Kelly, D.R. Lasher, and T.W. Phillips: Phys. Rev. C**4** (1971) 149.